Preferred Orientations in the Binding of 4'-Hydroxyacetanilide (Acetaminophen) to Cytochrome P450 1A1 and 2B1 Isoforms As Determined by ^{13}C- and ^{15}N-NMR Relaxation Studies

Timothy G. Myers,† Kenneth E. Thummel,‡ Thomas F. Kalhorn,‡ and Sidney D. Nelson*

Departments of Medicinal Chemistry and Pharmaceutics, University of Washington, Seattle, Washington 98195

Received October 8, 1993•

The widely used analgesic/antipyretic agent 4'-hydroxyacetanilide (acetaminophen, APAP) is oxidized by cytochromes P450 to a potent cytotoxin, *N*-acetyl-*p*-benzoquinone imine (NAPQI), and a nontoxic catechol, 3',4'-dihydroxyacetanilide (3-hydroxyacetaminophen, 3-OH-APAP). There are marked differences in the ratios of these two products formed from different isoforms of cytochrome P450. For example, the ratio of NAPQI to 3-OH-APAP formed by rat liver CYP1A1 was found to be approximately 3:1, whereas the ratio of the same two products formed by rat liver CYP2B1 was approximately 1:5. Investigations of the binding of APAP to CYP1A1 and CYP2B1 were carried out to assess the possibility that different preferred orientations of APAP in the active sites of these isoforms may, in part, by responsible for their different product selectivities. Although the spectral dissociation constants ($K_s \simeq 0.85$ mM) and UV-vis binding spectra (type I; absorption minimum $\simeq$ 420 nm, absorption maximum $\simeq$ 390 nm) were similar for interactions of APAP with the two P450 isoforms, NMR longitudinal relaxation times (T_1) of APAP nuclei were significantly different. Two isotopically substituted analogs of APAP, [2,3',5'-$^{13}C_3$]-4'-hydroxyacetanilide and 4'-hydroxyacet-[^{15}N]-anilide, were synthesized, and their binding to purified CYP1A1 and CYP2B1 was examined by NMR spectroscopy. Paramagnetic relaxation times (T_1p) for each of the labeled nuclei were calculated from the T_1 values obtained before (ferric) and after (ferrous-CO) treatment with $Na_2S_2O_4$ and CO. The Solomon-Bloembergen equation was then used to calculate distances of the isotopically labeled nuclei from the heme iron of each P450 isoform. The results were that the amide nitrogen approaches relatively close to the heme iron in CYP1A1 (3.64 ± 0.51 Å) whereas it is significantly further away (>4.5 Å) in CYP2B1. In contrast, the aryl carbon atoms ortho to the phenolic group of APAP approach closer to the heme iron of CYP2B1 (3.19 ± 0.12 Å) than to the heme iron of CPY1A1 (3.66 ± 0.30 Å). The results are consistent with the hypothesis that CYP1A1 produces NAPQI preferentially because of closer proximity of the heme iron to the amide nitrogen, whereas CYP2B1 produces 3-OH-APAP preferentially because of closer proximity of the heme iron to the phenolic oxygen in this isoform.

Introduction

Acetaminophen (4'-hydroxyacetanilide, *N*-acetyl-*p*-aminophenol, APAP) is a widely used analgesic and antipyretic agent that can cause hepatocellular injury and other toxicities in man and laboratory animals.[1-3] APAP is oxidized to the reactive metabolite and potent cytotoxin *N*-acetyl-*p*-benzoquinone imine (NAPQI) and to the nontoxic catechol 3-hydroxyacetaminophen (3',4'-dihydroxyacetanilide, 3-OH-APAP) by hepatic cytochromes P450.[4-6] The overall turnover rates for APAP have been found to vary widely among different forms of P450,[6-8] and of greater significance to the investigations described in this manuscript, there is a large variation in the ratio of formation rates of the two oxidation products.[6] For example, the ratio of NAPQI to 3-OH-APAP formed from rat liver CYP2B1 was approximately 1:5, whereas that ratio from rat liver CYP1A1 was approximately 3:1.

On the basis of these results, a mechanism was proposed in that NAPQI arose by hydrogen abstraction from the amide nitrogen of APAP (Figure 1, pathway A) whereas 3-OH-APAP arose by hydrogen abstraction from the phenolic group (Figure 1, pathway C). Thus, differences in rates of formation of NAPQI and 3-OH-APAP would be determined primarily by differences in orientation of the substrate, APAP, relative to a P450 ferryl-oxo complex. That the hypothetical mechanism involves hydrogen abstraction by a ferryl-oxo complex is supported by several studies that have been reviewed.[9-11]

On the basis of results of ^1H-NMR longitudinal relaxation rate measurements,[12] another mechanism has been proposed for the formation of both NAPQI (Figure 1, pathway B) and 3-OH-APAP (Figure 1, pathway C) from the phenoxy radical. Results of the ^1H-NMR relaxation studies indicated that the aromatic protons of APAP were oriented slightly closer to the heme iron in CYP1A1 than in CYP2B1, and only CYP1A1 was found to oxidize APAP to NAPQI at a measurable rate. Therefore, NAPQI apparently was formed from APAP because of the proximity of the phenolic end of APAP to the P450 heme iron. Formation of the catechol metabolite, 3-OH-APAP, was not monitored in that study. In support of the hypothesis that NAPQI was formed by initial abstraction of hydrogen from the phenol group, *ab initio* calculations indicated that hydrogen-radical abstraction from the phenolic oxygen is favored over hydrogen-radical abstraction from the amide nitrogen.[13]

However, these results do not easily explain the different

* Address correspondence to this author at the Department of Medicinal Chemistry, BG-20, University of Washington, Seattle, WA 98195.

† Present address: Laboratory of Molecular Pharmacology, Developmental Therapeutics Program, National Cancer Institute, Bethesda, MD 20892.

‡ Department of Pharmaceutics.

• Abstract published in *Advance ACS Abstracts*, February 15, 1994.

0022-2623/94/1837-0860$04.50/0

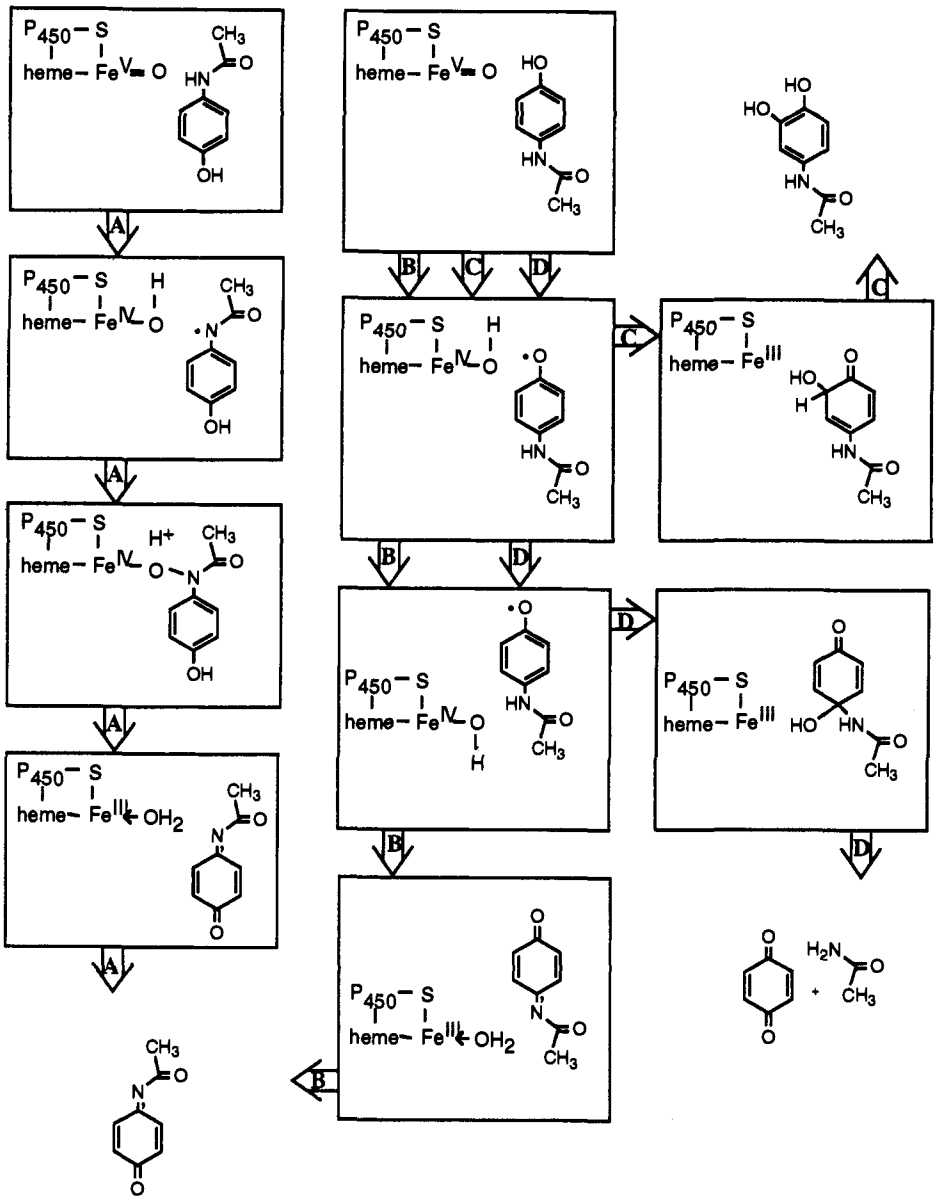

Figure 1. Mechanisms postulated for cytochrome-P450-mediated oxidation of APAP to NAPQI and 3-OH-APAP, and benzoquinone/acetamide. Pathway A leads to the production of NAPQI via initial oxidation at the amide nitrogen. Pathway B leads to the generation of NAPQI via initial oxidation at the phenol oxygen followed by reorientation of the phenoxy radical to facilitate hydrogen-radical abstraction from the amide nitrogen. Pathway C illustrates the mechanism for 3-OH-APAP formation via recombination of the ferryl oxy radical with the substrate. Pathway D illustrates the mechanism for formation of benzoquinone and acetamide via recombination of the ferryl oxy radical with the substrate at the C-1′ position. It should be noted that these mechanisms are quite speculative and that there are several alternatives, including mechanisms that involve electron transfers from heteroatoms or π-electron systems followed by proton losses.

ratios of NAPQI to 3-OH-APAP formed by different isoforms of P450. If the phenoxy radical is a common intermediate to both products, P450 must either perturb the relative contribution of different resonance forms of the APAP phenoxy radical or control the orientation of the radical and thereby dictate the region of its further interaction with the putative heme–oxo complex. Accordingly, P450 isoforms must differentially modulate the electron distribution of the phenoxy radical and/or its position with respect to the heme.

A problem with ^{1}H-NMR relaxation studies is that the intramolecular distance between the hydrogen nuclei of APAP is small compared to the intermolecular distance between these nuclei and the heme iron atom. This situation limits the use of ^{1}H-NMR experiments to detect, accurately, changes in substrate orientation from one isoform to another. Therefore, APAP analogs isotopically labeled with ^{13}C and ^{15}N were synthesized to obtain better estimates of the orientation of APAP at the active sites of purified rat liver CYP2B1 and CYP1A1 which exhibit opposite product selectivities for 3-OH-APAP and NAPQI.

Chemistry and NMR Studies

Isotopically enriched APAP analogs were synthesized by a published procedure[14] with modifications. The general procedure involved nitrosation of phenol followed by Raney nickel reduction of the nitrosophenol to the amine and finally acetylation of the amine with acetylimidazole freshly prepared from acetic acid and *N,N′*-carbonyldiimidazole. 4′-Hydroxyacet-[^{15}N]-anilide ([^{15}N]-APAP) was thereby prepared by using [^{15}N]$NaNO_2$, and [2,3′,5′-$^{13}C_3$]-4′-hydroxyacetanilide ([^{13}C]APAP) was prepared by using [2,6-$^{13}C_2$]phenol and [2-^{13}C]acetic acid.

Table 1. UV Binding Spectral Characteristics, Spectral Dissociation Constants,[a] and Catalytic Activities[b] of Rat Liver CYP2B1 and CYP1A1 for APAP

isoform	UV_{min}	UV_{max}	K_s (mM)	formation rates (nmol/nmol of P450/min) 3-OH-APAP	GS-APAP
CYP2B1	420	380	0.80 ± 0.03	0.63 ± 0.09	0.12 ± 0.02
CYP1A1	422	406	0.87 ± 0.06	0.41 ± 0.12	1.34 ± 0.13

[a] At saturating substrate concentrations, ΔA = 9.0 AU/nM for CYP2B1 and 6.7 AU/nM for CYP1A1. Using a dual beam spectrophotometer, both cells contained 1 μM P450 and 20 μg/mL DLPC in 100 mM potassium phosphate, pH 7.4, buffer. A concentrated solution of APAP in DMSO was added to the sample cuvette, and DMSO was added to the reference cuvette. $A_{max} - A_{min}$ was plotted against the final concentration of substrate and analyzed by nonlinear, least-squares regression to arrive at a value for K_s, the concentration of APAP producing a half-maximal UV absorbance (ΔA). [b] Formation rates were obtained as described in the Experimental Section at saturating substrate concentrations (10 mM).

Overall yields of the crystallized product were approximately 50% by this method.

NMR experiments were conducted at 24 ± 2 °C using APAP substrate concentrations that were saturating (~10 mM) with cytochrome P450 enzyme concentrations ranging from approximately 1 to 10 μM. T_1 values were measured from each atom enriched in ^{15}N and ^{13}C before and after conversion of the P450 to its reduced, CO complex. The paramagnetic relaxation times, T_1p, were calculated, and the Solomon–Bloembergen equation[15,16] was used to estimate the distances of the probe nuclei from the paramagnetic heme center of the P450 isoform as described in detail in the Experimental Section.

Results and Discussion

The binding of APAP to CYP2B1 and CYP1A1 was spectrally observed by UV difference spectra, and the results are tabulated (Table 1). APAP caused a type I spectral change with both isoforms. The effect was saturable, and the calculated K_s values for each enzyme were comparable. These K_s values were used to calculate the mole fraction of acetaminophen that was active-site bound (P_M). The formation rates for 3-OH-APAP and GS-APAP (3′-glutathion-*S*-ylacetaminophen, as a reflection of NAPQI) under saturating substrate conditions (10 mM) gave relative turnover numbers that were essentially identical to those previously reported at substrate concentrations of 1 mM.[6]

Examples of spectra obtained during acquisition of T_1 data for [^{15}N]APAP and [^{13}C]APAP at concentrations of 10 mM provide a dynamic view of the relaxation of the ^{15}N- and ^{13}C-nuclei over time (Figures 2 and 3). The ferric form of CYP1A1 caused a decrease in the T_1 for all of the observed nuclei of acetaminophen relative to the T_1 after reduction to the diamagnetic, ferrous form (Table 2). CYP2B1 had a detectable effect on only the aryl C-3′(5′) nuclei of acetaminophen and not on the acetyl group carbon (C-2) or the amide nitrogen.

Nucleus to heme iron distances (Table 3) were calculated as described in the Experimental Section. Note that the absolute distances reported here are dependent on the electronic correlation time for the paramagnetic complex. The value used was determined for $P450_{cam}$, which, like mammalian forms of P450, contains a protoporphyrin IX–iron complex and a cysteinyl sulfur as the iron's fifth ligand. Important features of these calculations are that the amide nitrogen atom and the acetyl group carbon atom

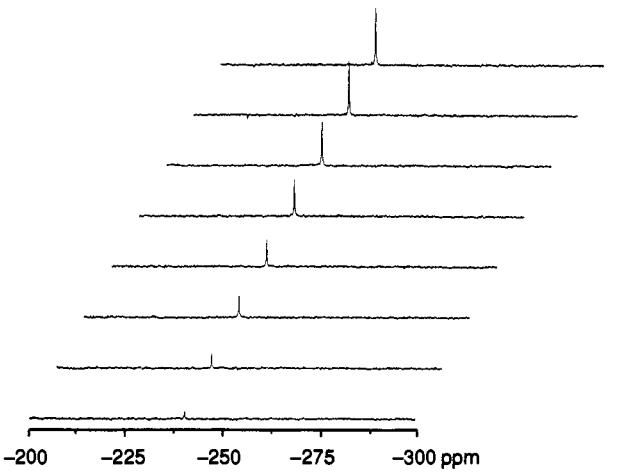

Figure 2. Spectra obtained during a T_1 determination in the reaction of [^{15}N]APAP with CYP1A1. The spectrometer had a proton frequency of 300 MHz. The saturation recovery method used τ values of 1, 2, 3, 4, 6, 8, 12, and 15 s. Resonance shift assignments are given in the Experimental Section.

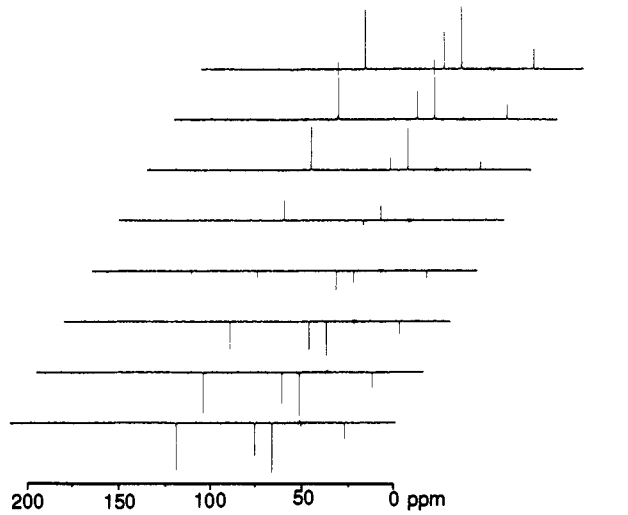

Figure 3. Spectra obtained during a T_1 determination in the reaction of [^{13}C]APAP with CYP1A1. The spectrometer had a proton frequency of 300 MHz. The inversion recovery method used τ values of 0.094, 0.188, 0.375, 0.750, 1.5, 3, 6, and 12 s. Resonance shift assignments are given in the Experimental Section.

of APAP are significantly further away from the heme iron of CYP2B1 than from that of CYP1A1, whereas the C-3′(5′) aryl carbon atoms of APAP are nearer to the heme iron of CYP2B1 than to that of CYP1A1.

It should be noted that there was less variation between preparations in the measurements of relaxation times (and therefore calculated distances) of probe nuclei closest to the paramagnetic heme center than those further away. For example, the C-2 acetyl carbon atom was more difficult to accurately locate than either the amide nitrogen or the aryl carbon atoms in CYP1A1 (Tables 2 and 3). The reasons for this are not entirely clear. In spite of this difference in accuracy, there were significant differences in the relaxation rates for all of the probe nuclei of APAP between the two different P450 isoforms.

Using the results in Table 3, models of the interaction of APAP with the protoporphyrin IX heme iron were generated (Figures 4 and 5). For ease of viewing, the substrate is depicted perpendicular to the heme moiety, although it may orient parallel to the heme moiety as well. The active sites of both CYP1A1 and CYP2B1 apparently

Table 2. Longitudinal Relaxation Times of APAP Nuclei in the Presence of the Fe^{3+}- or (Fe^{2+}–CO)-P450

isoform	heme state[a]	relaxation time, T_1 (s)		
		^{13}C-2	^{15}N	^{13}C-3′, ^{13}C-5′
CYP2B1[b]	Fe^{3+}		4.73 ± 0.57	
	Fe^{2+}–CO		4.58 ± 0.75	
CYP2B1[c]	Fe^{3+}	2.30 ± 0.13		1.12 ± 0.01
	Fe^{2+}–CO	2.37 ± 0.09		1.25 ± 0.03
CYP2B1[d]	Fe^{3+}	2.31 ± 0.03		1.11 ± 0.01
	Fe^{2+}–CO	2.35 ± 0.05		1.18 ± 0.01
CYP1A1[e]	Fe^{3+}		7.29 ± 0.61	
	Fe^{2+}–CO		8.24 ± 0.45	
CYP1A1[f]	Fe^{3+}	2.21 ± 0.04		1.10 ± 0.02
	Fe^{2+}–CO	2.34 ± 0.06		1.16 ± 0.02
CYP1A1[g]	Fe^{3+}	2.32 ± 0.02		1.16 ± 0.01
	Fe^{2+}–CO	2.42 ± 0.04		1.22 ± 0.01

[a] Fe^{3+} corresponds to native enzyme, and Fe^{2+}–CO is the same solution after treatment with carbon monoxide and $Na_2S_2O_4$ as described in the Experimental Section. [b-g] Enzyme concentrations (μM): 10, 1.0, 0.57, 2.4, 1.2, and 1.3, respectively. The results are from four or more determinations of T_1 values with each enzyme preparation and each stable isotope analog. Values from two different enzyme preparations of each isoform are given for some nuclei. Not enough enzyme was available to carry out additional studies.

Table 3. Calculated Fe–Nucleus Distances

isoform	distance (Å)[a]		
	^{13}C-2	^{15}N	^{13}C-3′, ^{13}C-5′
CYP2B1		>4.52[b]	
CYP2B1	>4.86[b]		3.19 ± 0.12
CYP2B1	>4.82[b]		3.17 ± 0.07
CYP1A1		3.64 ± 0.51	
CYP1A1	4.08 ± 0.30		3.66 ± 0.30
CYP1A1	4.38 ± 0.35		3.77 ± 0.17

[a] Distances were calculated using the Solomon–Bloembergen equation as described in the Experimental Section. Each distance is based on the corresponding T_1 values from Table 2. Values following ± represent experimental error λ(r) as described in the Experimental Section. [b] Value corresponds to the limit of detection, as described in the Experimental Section. Refer to Table 2 for additional details of the enzyme preparations used.

have a high area/depth ratio, based on studies with other substrates.[17,18] Our ability to model the interaction of APAP and the heme iron of CYP2B1 was limited because only one distance measurement could be ascertained within detection limits: that of the C-3′(5′) of APAP to the heme iron (Table 3, Figure 4). However, the results clearly indicate that the amide group is at a greater distance from the heme iron compared to the phenolic end of the molecule. In contrast, a more exact model of the orientation of APAP around the heme iron of CYP1A1 was possible because three distances could be measured (Table 3, Figure 5). The amide nitrogen and the C-3′(5′) of APAP were calculated to be about equidistant from the heme iron in this isoform.

Several kinds of studies have demonstrated that regioselectivity in product formation by cytochromes P450 is controlled by both substrate-dependent parameters (e.g., hydrogen-bonding sites, intermediate-radical stability) and constraints imposed by the active-site topology of the P450s.[19-27] ^{1}H-NMR relaxation studies of cytochromes P450 were used for the first time in an investigation of binding orientations of acetanilide to two different rabbit isoforms of P450,[28] and this has recently been extended to the two rat orthologs.[29] The results indicated that differences in substrate orientation at the active site of different P450 isoforms paralleled differences in product selectivity. Our NMR results also indicate that differences in catalytic activity and product selectivity of CYP2B1

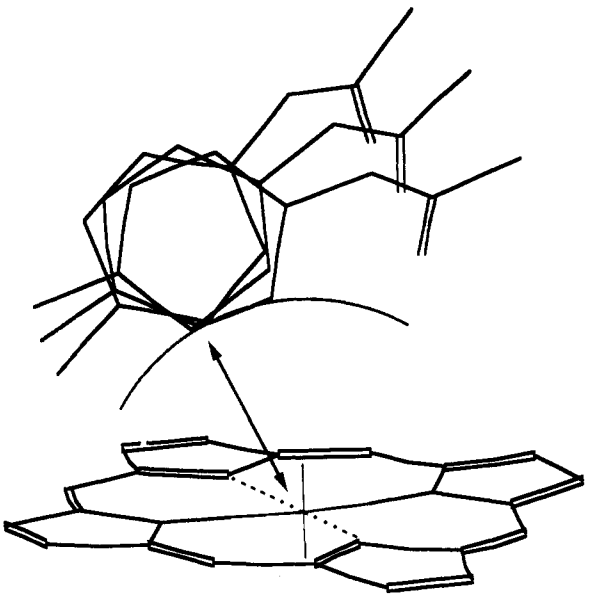

Figure 4. Scale drawing of the atomic positions of APAP relative to heme in CYP2B1. Arrows indicate probe atoms used in docking the substrate to the heme. An approach that is perpendicular to the heme is shown for clarity, although the substrate and the heme may be in parallel planes. Only one distance was determined precisely—that between the C-3′ and the Fe (double-headed arrow). However, the N and C-2 atoms are significantly farther from the Fe in CYP2B1 than in CYP1A1 (see Figure 5).

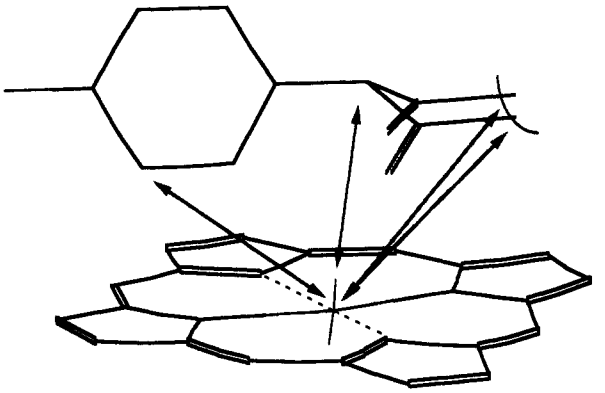

Figure 5. Scale drawing of the atomic positions of APAP relative to heme in CYP1A1. The double-headed arrows indicate the probe atoms used in docking the substrate to the heme. All three distances were measurable, though there was more uncertainty about the C-2 acetyl methyl-group position as indicated. Using the three distances determined with CYP1A1 (double-headed arrows), it is easier to define the orientation of APAP. The position of the aromatic ring is fixed by triangulation of the heme iron, the C-3′ carbon, and the nitrogen atom. Then, to bring the C-2 (acetyl) carbon to the calculated distance, the C-1–N bond was rotated.

and CYP1A1 for APAP parallel differences in APAP-binding orientation, inasmuch as 3-OH-APAP formation rates are about the same for both isoforms wherein the distance of nearest approach of the heme iron to the phenolic group of APAP is nearly equal, whereas CYP1A1 forms NAPQI approximately 10 times faster than CYP2B1, consistent with the finding that the amide nitrogen of APAP approaches significantly closer to the heme iron of CYP1A1 compared to that of CYP2B1.

In a recent NMR study,[30] ^{19}F-NMR relaxation rates were measured to determine the distance between the 9-fluoromethyl group of bound 9-(fluoromethyl)camphor to the heme iron of CYP101 ($P450_{cam}$). It is significant that the absolute distances obtained between the heme iron and

the oxidation sites on the camphor substrate are comparable to the distances found in our studies between the heme iron and the putative oxidation sites on APAP. Of course, it is likely that the active site of $P450_{cam}$ is much more restricted than that in CYP2B1 and CYP1A1, but this does not mean that substrates do not orient preferentially within the active site of these mammalian isoforms.

The investigation of (fluoromethyl)camphor is particularly enlightening because the distances obtained by the NMR measurements compared closely with those obtained by X-ray crystallography. Our results predict distances of 3–4 Å between the nuclei in APAP that putatively undergo oxidation and the heme iron of P450. Results from X-ray crystallography studies of the camphor–$P450_{cam}$ complex show a distance of 4.2 Å between the C-5 carbon that becomes oxidized and the $P450_{cam}$ heme iron,[31] while the ^{19}F-NMR results predict a distance of about 3.4 Å (as estimated from data in ref 30). It should be noted that the distance values generated by NMR T_1 experiments represent the *shortest* distance between the paramagnetic heme iron and the nuclei of the substrate. Binding and debinding of substrate to the P450 active site is a dynamic process, thus the *average* distance likely will be greater than that measured by NMR T_1 relaxation rates.

The distances determined in all of these studies necessarily have been carried out on nonoxygenated P450s, but the distances allow room for oxygen binding to the heme iron. Thus, these NMR studies do not necessarily provide information about the more relevant orientation of substrates in the catalytically active oxo–ferryl form of the enzymes. However, in only one case so far has it been determined that a substrate of $P450_{cam}$ undergoes substantial reorientation in going from the ferric to the oxo–ferryl complex.[32] We believe that this is because the substrate, thiocamphor, contains the thiocarbonyl group, which is a relatively strong π-field ligand, that orients toward the heme iron in the $P450_{cam}$ ferric state. It loses this interaction when the enzyme is reduced and binds oxygen, and the thiocarbonyl group then hydrogen bonds to the same tyrosine hydroxyl group to which the carbonyl oxygen of camphor binds. Inasmuch as the APAP structure does not contain any strong liganding groups, we believe that such binding and reorientation is unlikely.

On the basis of the distance data that were obtained for isotopically labeled APAP (Table 3, Figure 4), we conclude that the phenolic end of the molecule, on average, approaches nearer to the heme iron in CYP2B1 than the amide group. This orientation may facilitate 3-OH-APAP formation and is consistent with the greater formation rate of 3-OH-APAP than NAPQI by this isoform. We also conclude that, on average, the amide group approaches nearer to the heme iron in CYP1A1 than does the phenolic group (which must be at least 0.5 Å farther removed from the heme iron than C-3′ and C-5′), though both regions of the molecule are within a distance where oxidation may occur. This orientation (Figure 5) may facilitate NAPQI formation and is consistent with the greater formation rate of NAPQI by this isoform. It is noteworthy that 3-OH-APAP is formed at a significant rate by both CYP2B1 and CYP1A1 and that their rank order with respect to formation rate matches their rank order with respect to distance measurements of C-3′(5′) to the heme iron.

Thus, we conclude that the orientation of APAP at the active site of cytochromes P450 is a factor in the determination of product selectivity even though we do not know what residues are involved in the orientation. From a theoretical standpoint,[13] it can be argued that abstraction of a hydrogen radical from the phenolic group is so much more thermodynamically favorable than abstraction from the amide nitrogen that the latter reaction would not occur. However, it is known that some arylamides such as 4′-ethoxyacetanilide[33] and 2-acetylaminofluorene[34,35] are hydroxylated at the amide nitrogen and that cytochromes of the CYP1A family are most active. It also has been determined by molecular orbital methods that removal of a hydrogen radical from the amide nitrogen of APAP by a P450-like oxidant is thermodynamically possible.[36]

This is not to say either that purely substrate-dependent electronic factors may not play a role in product selectivity or that NAPQI cannot be formed by initial abstraction of hydrogen from the phenolic group. It has been postulated[13,37] that the phenolic radical could essentially undero a second site-mediated hydrogen abstraction to form NAPQI (Figure 1, pathway B). In addition, small amounts of *p*-benzoquinone that are formed may arise by recombination of the oxy radical at the ipso carbon atom followed by elimination of acetamide (Figure 1, pathway D), another known metabolite of acetaminophen.[38] Such a reaction would require that the initial APAP radical be stable and mobile enough in a P450 active-site radical cage so that a P450 oxy radical recombines at the amide end of the aromatic ring para to the phenolic group from which the oxy radical was formed. Recent investigations[39] have provided evidence for such a possibility, inasmuch as oxygen from molecular oxygen is incorporated into the *p*-benzoquinone product, though it is formed at rates only one-twentieth that of NAPQI.

Conclusion

In summary, ^{13}C- and ^{15}N-NMR T_1 relaxation studies have provided evidence that the orientation of APAP at the active sites of rat liver CYP2B1 and CYP1A1 are different and that these results are consistent with the product selectivities of these two isoforms. However, we cannot rule out the possibility that, in part, a common APAP phenoxy radical partitions to different products in different ratios dependent on P450 active-site dynamics.

Experimental Section

Chemicals. Dilauroylphosphatidylcholine (DLPC), NADPH, phenylmethylsulfonyl fluoride (PMSF), EDTA, and FMN were purchased from Sigma Chemical Co. (St. Louis, MO). The buffer solution used throughout the NMR experiments consisted of 0.1 M potassium phosphate, pH 7.4, and 25% glycerol. Chemicals used in the synthesis of labeled APAP were obtained from Aldrich Chemical Co. (Milwaukee, WI) unless stated otherwise.

Synthesis of [^{15}N]APAP and [^{13}C]APAP. Isotopically enriched APAP analogs were synthesized according to a published procedure[14] with modifications. The stable isotopes [^{15}N]$NaNO_2$, [2,6-$^{13}C_2$]phenol, and [2-^{13}C]acetic acid were purchased from Cambridge Isotope Laboratories (Woburn, MA). Phenol, 0.5 g (5.31 mmol), was dissolved in H_2O with 0.25 g of NaOH and then cooled to 5 °C. After 0.46 g (6.67 mmol) of $NaNO_2$ and 0.55 mL of 30% NH_4OH were added, concentrated H_2SO_4 (0.55 mL) was added dropwise (5–10 min). The nitrosophenol product was isolated by filtration and further recovered from the mother liquor after cooling on ice. The air-dried nitrosophenol was dissolved in absolute EtOH. Raney nickel (10 g wet, neutral slurry) and 2 mL of concentrated HCl were added, and the mixture was refluxed for 1 h. After the first 40 min, an additional 0.5 mL of HCl was added. The cooled ethanol mixture was filtered through Celite. After the neutral to slightly acid pH of the filtrate was confirmed, a solution of acetylimidazole in tetrahydrofuran was slowly added. Acetylimidazole was prepared from a solution of

acetic acid (0.64 g, 11.4 mmol) in freshly distilled tetrahydrofuran by adding *N,N'*-carbonyldiimidazole (1.7 g, 10.5 mmol). The acetylation was complete within 3 h, after which excess acetylimidazole was destroyed by the addition of 1 mL of concentrated HCl. After 30 min, ethanol was removed *in vacuo* and the residue partitioned between H_2O and ethyl acetate. Combined ethyl acetate extracts were dried over Na_2SO_4. The drying agent was removed by filtration, and the remaining solvent was removed *in vacuo*. The acetaminophen product was further purified on a silica gel (70–230 mesh) column eluted with ethyl acetate. The overall yield was 50%.

Both labeled compounds were characterized by mass spectrometry as well as by NMR. **[^{15}N]APAP**: EI/MS (direct probe) m/z 152 $[M]^{\cdot+}$, 110 $[M - COCH_2]^{\cdot+}$ (base peak); ^{15}N NMR (aqueous buffer, proton decoupled) δ 240 (NO_3^-). **[^{13}C]APAP**: EI/MS (direct probe) m/z 154 $[M]^{\cdot+}$, 111 $[M - [^{13}C]OCH_2]^{\cdot+}$ (base peak); ^{13}C NMR (aqueous buffer, proton decoupled) (TMS) δ 175 (C-1), 156 (C-4'), 132 (C-1'), 127 (C-2'), 118 (C-3'), 23 (C-2). Isotopic enrichment was 96% for [^{15}N]APAP and 98% for [^{13}C]-APAP as determined by mass spectrometry.

Enzymes. CYP1A1 was purified from liver microsomes isolted from 3-methylcholanthrene (3MC)-induced, juvenile, male Sprague–Dawley rats following a published method.[40] The purification of cytochrome CYP2B1 from phenobarbitol (PB)-induced juvenile, male Sprague–Dawley rats was accomplished by a combination of published procedures. Microsomes were solubilized in buffer containing 0.2% Emulgen 911, 10 mM potassium phosphate, pH 7.7, 20% glycerol, 1 mM EDTA, 1 mM dithiothreitol (DTT), 0.1 mM PMSF, and 5 μM flavin mononucleotide (FMN). Soluble protein was applied to a DEAE-Sepharose column and washed exhaustively with the same solubilization buffer. A protein fraction containing CYP2B1 was eluted with a step gradient to 50 mM potassium phosphate, pH 7.7. Cytochrome P450 reductase and cytochrome b_5 were eluted with a linear 0–0.5 M KCl gradient in 50 mM potassium phosphate buffer. The pooled CYP2B1 fraction was diluted 2:3 (v/v) with 10 mM potassium phosphate, pH 7.4, 20% glycerol, 0.4% sodium cholate, 1 mM EDTA, 1 mM DTT, 0.1 mM PMSF, and 0.5 M NaCl, and applied to an octyl-Sepharose column. A highly enriched CYP2B1 fraction was isolated after chromatography as previously described.[41] Final purification was achieved with chromatography on hydroxyl apatite.[42] Protein concentration and total P450 content were determined by published methods.[43,44] Specific contents were 14 and 12 nmol of P450/mg of protein for CYP1A1 and CYP2B1, respectively. Preparations were stored in 50 or 100 mM potassium phosphate buffer containing 25% glycerol at −70 °C until used.

Spectral Dissociation Constants. UV difference spectra were determined using a Hewlett-Packard HP8450 dual beam UV spectrophotometer. Purified enzymes were reconstituted with freshly sonicated DLPC for 20 min at room temperature before being diluted with 0.1 M potassium phosphate buffer (final concentration 1 μM P450 and 30 μg/mL DLPC). Aliquots of acetaminophen dissolved in spectral grade dimethyl sulfoxide (DMSO) were added to one cuvette, and equal volumes of DMSO were added to the reference cuvette. After each addition, the samples were mixed by inversion and allowed to equilibrate for 1 min. Calculated ΔA ($\lambda_{max} - \lambda_{min}$) values were corrected for dilution and analyzed by nonlinear least-squares regression using a saturable binding model to arrive at the spectral dissociation constant, K_s.

Enzyme Activity Assays. Isozyme incubations contained the appropriate P450 isoform (1 μM), purified rat liver NADPH–cytochrome P450 reductase (1.5 μM), DLPC (30 μM), NADPH (0.5 mM), glucose-6-phosphate (10 mM), glucose-6-phosphate dehydrogenase (1 IU/mL), gluathione (GSH) (10 mM), and [^{14}C]-APAP (10 mM, specific activity 1.5 mCi/mmol) in 1.0 mL of 0.05 M potassium phosphate buffer, pH 7.4. After a 3-min preincubation at 37 °C, reactions were initiated by addition of NADPH. The incubations were allowed to proceed for 20 min at 37 °C and terminated by freezing in dry ice–actone. After thawing, the proteins were precipitated by the addition of ice-cold methanol (1 mL) and centrifuged (2000g, 20 min). The cold carriers, GS-APAP and 3-OH-APAP, were added to each sample to give final concentration of ca. 0.05 mM. After evaporation of the methanol under N_2 (40 °C), the samples were lyophilized. The buffer salts were precipitated with methanol (5 mL) and removed by centrifugation. The organic solvent was evaporated under N_2, and the samples were stored at −80 °C prior to analysis by HPLC.

HPLC analysis was performed on a Waters μBondapak C_{18} column (3.9 mm × 30 cm) with UV detection at 254 nm. The mobile phase consisted of 92% 0.075 M KH_2PO_4 (1% in acetic acid) and 8% methanol pumped isocratically at a flow rate of 1.0 mL/min. The column was flushed with 100% methanol between injections. Under these conditions, the following retention times were obtained for synthetic standards: 3-OH-APAP, 7.0 min; APAP, 10.5 min; GS-APAP, 17 min. Fractions were collected at 0.5- or 1-min intervals bracketing the appropriate retention times of the metabolites, and the radioactivity was measured by liquid scintillation counting (15 mL of Aquasol-2).

NMR Studies. NMR measurements were taken on a Varian VXR-300 FT-NMR spectrometer with a proton frequency of 300 MHz. Samples included 10% D_2O for frequency lock and were contained in a standard 5-mm NMR tube. The probe was maintained at ambient temperature (24 ± 2 °C) which did not change more than a few tenths of a degree over all the measurements of any particular enzyme sample. An inversion-recovery pulse sequence was used for ^{13}C, with a preacquisition delay of $4T_1$. A saturation-recovery pulse sequence was used for ^{15}N. For both nuclei, seven τ values were used. Attempts to degas the solutions containing P450 (Ar and N_2 purging, evacuation) did not result in a significant increase in T_1 (except when the increase could be attributed to degradation of P450–Fe^{3+}). Therefore, the contribution of dissolved oxygen to T_1 was considered to be negligible in the present investigation.

T_1 was measured before and after conversion of the P450 to its reduced, CO complex. APAP (2 mg) was dissolved in acetone in a Reacti-Vial (Pierce Chemical Co., Rockford, IL). The solvent was removed by a stream of N_2, and the residue was dissolved in buffer and D_2O before adding cytochrome P450 (0.5–5 nmol) in buffer. The P450 was used immediately after thawing. Final volumes ranged from 0.5 to 0.7 mL. Measurement of $T_1(Fe^{3+})$ was completed within the next 1–3 h. The solution was then transferred to a microfuge test tube and bubbled with CO for 1 min. Sodium dithionite (final concentration 0.1 mM) was added as a solution in degassed H_2O (3.7 g/L) prepared immediately prior to use. Reduction of the P450 was complete in less than 30 min as determined by UV measurements and by a stabilization of the T_1 values. Measurement of $T_1(Fe^{2+}–CO)$ was conducted within the next 1–3 h. Thermal degradation of the P450 over the course of the experiments was less than 10% as determined by UV assay of a prallel sample maintained at the same temperature. Cytochrome P420 accumulation was not apparent.

The paramagnetic relaxation time T_1p was calculated from the average ($n \geq 4$) $T_1(Fe^{3+})$ and the average $T_1(Fe^{2+}–CO)$ according to the equation

$$1/T_1p = 1/T_1(Fe^{3+}) - 1/T_1(Fe^{2+}–CO) \quad (1)$$

which defines T_1p as the decrease in relaxation time (or the increase in the rate) attributable to the paramagnetic (Fe^{3+}) ion.

Distance Calculations. The Solomon–Bloembergen equation[15,16] and the experimentally determined value of T_1p were used to estimate the distance of the bound probe nuclei from the paramagnetic center of the isoform. The distance r, in angstroms, is given by

$$r = C(T_1pP_Mqf(\tau_c))^{1/6} \quad (2)$$

The constant C incorporates the magnetic susceptibility of the probe nuclei and the paramagnetic center. The heme iron was assumed to be high spin, based on the UV binding spectra (see below). Values of C were 378 for ^{15}N and 512 for ^{13}C. The full definitions for C and $f(\tau_c)$ and eq 2 can be found elsewhere.[45] P_M is the mole fraction of bound substrate, and q is the coordination number. We have assumed a coordination number of 1.0 and that P_M = [enzyme]/K_s.

The T_1 measurement overwhelmingly reflects the probe molecules in bulk solution, not the probe actually bound to the enzyme. To the extent that the probe was alternately bound to the enzyme near the paramagnetic center and able to exchange with the probe molecules in bulk solution, an effect of the paramagnetic center on the probe could be observed. Thus, the

condition that the substrate be in, so-called, "fast exchange" was necessary for the observation of a T_1p since the molar ratio of enzyme to substrate (10^{-4}) in these experiments was small.[46] This phenomenon is expressed in the following equation:[47]

$$T_1p^{-1} = P_M q/(T_{1M} + t_m) \quad (3)$$

where T_{1M} is the relaxation time of the probe nucleus in the first coordination sphere of the paramagnetic center and t_m is the inverse of the chemical exchange rate and can be thought of as the residence time of the probe nucleus in the first coordination sphere of the paramagnetic center. When $t_m \ll T_{1M}$, i.e., when the relaxation rate of the bound probe is slower than the chemical exchange between the bound and bulk populations, fast exchange is in effect and eq 3 can be simplified so that $T_{1M} = T_1pP_Mq$, as represented in eq 2.

Exchange limitation can diminish or nullify the observed T_1p even when a significant paramagnetic effect is present. In our experiments, the ratio of unbound substrate to bound substrate is at least 100:1. Thus, we would not have been able to observe an effect on T_1 if t_m were not considerably less than T_{1M}. Observed values of T_1pP_Mq were greater than 10^{-2} s, meaning that t_m, the lifetime of the bound substrate, would have to be as large as 10^{-4} s to be significant. A t_m of 10^{-4} s or greater seems unlikely for a substrate with a dissociation constant on the order of 1 mM, as in the present case. In contrast, exchange-limited T_1p has been reported where T_1pP_Mq products on the order of 10^{-4} s or less were found to be exchange limited.[48]

The correlation time τ_c for $P450_{cam}$, determined by the frequency dependence of ^{19}F T_1 in 9-(fluoromethyl)camphor, is 6.15×10^{-13} s.[30] Since the electronic correlation time was found to be the only significant contributor to τ_c, we used the same value for all of our distance calculations. Thus, $f(\tau_c)$ was equal to 4.57×10^{-12} s for both ^{13}C and ^{15}N nuclei observed at 7.05 T. It should be noted that since τ_c^{-1} was within 1 order of magnitude of ω_s, the resonance frequency of the unpaired electron (1.24×10^{12} at 7.05 T), then the values of $f(\tau_c)$ and r were particularly sensitive to the chosen value of τ_c.

Error Analysis. Experimental error associated with the distance estimates was calculated using a method for propagation of error through a nonlinear equation.[49] The error with respect to r was determined by partial derivatives of the Solomon–Bloembergen equation with respect to the relaxation rate variables. The confidence limits associated with r are calculated as $\lambda(r)$, the sum of the variance of each T_1 value multiplied by their partial derivative, as shown below.

$$r = bT_1p^{1/6}$$

where

$$b = C(P_Mq f(\tau_c))^{1/6}$$

and

$$T_1p = 1/(1/T_1(Fe^{3+})) - 1/T_1(Fe^{2+}\text{–CO})$$

Then,

$$\frac{\partial r}{\partial T_1(Fe^{3+})} = \frac{bT_1p^{7/6}}{6T_1(Fe^{3+})}$$

and

$$\frac{\partial r}{\partial T_1(Fe^{2+}\text{–CO})} = \frac{-bT_1p^{7/6}}{6T_1(Fe^{2+}\text{–CO})}$$

Thus,

$$\lambda^2(r) = \left(\frac{\partial r}{\partial T_1(Fe^{3+})}\right)^2 \lambda^2(T_1(Fe^{3+})) + \left(\frac{\partial r}{\partial T_1(Fe^{2+}\text{–CO})}\right)^2 \lambda^2(T_1(Fe^{2+}\text{–CO}))$$

The square root of $\lambda^2(r) = \lambda(r)$ and gives the confidence interval of the measured variables or an approximate SD. Using this method, b values for each of the measurable distances were CYP2B1 ^{13}C-3′(5′), 0.259 and 0.252; CYP1A1 ^{15}N, 0.386; CYP1A1 ^{13}C-2, 0.269 and 0.253; and CYP1A1 ^{13}C-3′(5′), 0.213 and 0.226.

Limit of Detection. The limit of detection was calculated using the T value for Fe^{2+}–CO and the standard deviation associated with the nonlinear least-squares regression estimate of that value. Our approach was to determine the value of T_1 that would be considered a statistically significant decrease from the T_1 corresponding to the Fe^{2+}–CO state. Using this value, it was then possible to determine the largest measurable T_1p and ultimately the largest value of r that would be measurable under the conditions of that experiment. Using the Student's t distribution, at $p = 0.90$ and $n = 8$, a significant difference between two means is 0.51SD. Therefore, r at the limit of detection was calculated using the equations above by setting $T_1(Fe^{3+}) = T_1(Fe^{2+}\text{–CO})_{obs} - 0.51SD$.

Modeling. Modeling of APAP orientation of the active site was aided by Alchemy II software for the Macintosh (Tripos, St. Louis, MO).

Acknowledgment. This work was supported by National Institutes of Health Grant Nos. GM32165 and GM25418 (S.D.N.) and by Training Grant No. GM07750 (T.G.M.). We also wish to thank Ms. Cindy Chernoff for her valuable technical assistance.

References

(1) Hinson, J. A. Biochemical Toxicology of Acetaminophen. *Rev. Biochem. Toxicol.* **1980**, *2*, 103–130.
(2) Nelson, S. D. Molecular Mechanisms of the Hepatotoxicity Caused by Acetaminophen. *Semin. Liver Dis.* **1990**, *10*, 267–278.
(3) Vermeulen, N. P. E.; Bessems, J. G. M.; van de Straat, R. Molecular Aspects of Paracetamol-Induced Hepatotoxicity and Its Mechanism-Based Prevention. *Drug Metab. Rev.* **1992**, *24*, 367–407.
(4) Dahlin, D. C.; Nelson, S. D. Synthesis, Decomposition Kinetics and Preliminary Toxicological Studies on Pure *N*-Acetyl-*p*-Benzoquinone Imine, A Proposed Toxic Metabolite of Acetaminophen. *J. Med. Chem.* **1982**, *25*, 8885–8886.
(5) Dahlin, D. C.; Miwa, G. T.; Lu, A.-Y. H.; Nelson, S. D. *N*-Acetyl-*p*-Benzoquinone Imine: A Cytochrome P-450-Mediated Oxidation Product of Acetaminophen. *Proc. Natl. Acad. Sci. U.S.A.* **1984**, *81*, 1327–1331.
(6) Harvison, P. J.; Guengerich, F. P.; Rashed, M. S.; Nelson, S. D. Cytochrome P-450 Isozyme Selectivity in the Oxidation of Acetaminophen. *Chem. Res. Toxicol.* **1988**, *1*, 47–52.
(7) Morgan, E. T.; Koop, D. R.; Coon, M. J. Comparison of Six Rabbit Liver Cytochrome P-450 Isozymes in Formation of a Reactive Metabolite of Acetaminophen. *Biochem. Biophys. Res. Commun.* **1983**, *112*, 8–13.
(8) Raucy, J. L.; Lasker, J. M.; Lieber, C. S.; Black, M. Acetaminophen Activation by Human Liver Cytochromes P450IIE1 and P450IA2. *Arch. Biochem. Biophys.* **1989**, *271*, 270–283.
(9) Guengerich, F. P.; Macdonald, T. L. Chemical Mechanisms of Catalysis by Cytochromes P-450: A Unified View. *Acc. Chem. Res.* **1984**, *17*, 9–16.
(10) Ortiz de Montellano, P. R. Cytochrome P-450 Catalysis: Radical Intermediates and Dehydrogenation Reactions. *Trends Pharmacol. Sci.* **1989**, *10*, 354–359.
(11) White, R. E. The Involvement of Free Radicals in the Mechanisms of Monooxygenases. *Pharmacol. Ther.* **1991**, *49*, 21–42.
(12) van de Straat, R.; de Vries, J.; de Boer, H. J. R.; Vromans, R. M.; Vermeulen, N. P. E. Relationship Between Paracetamol Binding to and Its Oxidation by Two Cytochrome P450 Isozymes – A Proton Nuclear Magnetic Resonance and Spectrophotometric Study. *Xenobiotica* **1987**, *17*, 1–9.
(13) Koymans, L.; Van Lenthe, J. H.; van de Straat, R.; Donne-op den Kelder, G. M.; Vermeulen, N. P. E. A Theoretical Study on the Metabolic Activation of Paracetamol by Cytochrome P-450: Indications for a Uniform Mechanism. *Chem. Res. Toxicol.* **1989**, *2*, 60–66.
(14) Hinson, J. A.; Nelson, S. D.; Gillette, J. R. Metabolism of [*p*-^{18}O]-Phenacetin: The Mechanisms of Activation of Phenacetin to Reactive Metabolites in Hamsters. *Molec. Pharmacol.* **1979**, *15*, 419–427.
(15) Solomon, I. Relaxation Processes in a System of Two Spins. *Phys. Rev.* **1955**, *99*, 559–565.
(16) Bloembergen, N. Proton Relaxation Times in Paramagnetic Solutions. *J. Chem. Phys.* **1957**, *27*, 572–573.
(17) Thakker, D. R.; Levin, W.; Yagi, H.; Yeh, H. C.; Ryan, D. E.; Thomas, P. E.; Conney, A. H.; Jerina, D. M. Stereoselective Metabolism of the (+)-(*S,S*)- and (−)-(*R,R*)-Enantiomers of *trans*-3,4-Dihydroxy-3,4-dihydrobenzo[c]phenanthrene by Rat and Mouse Liver Microsomes and by a Purified and Reconstituted Cytochrome P450 System. *J. Biol. Chem.* **1986**, *261*, 5404–5413.

(18) Swanson, B. A.; Dutton, D. R.; Lunetta, J. M.; Yang, C. S.; Ortiz de Montellano, P. R. The Active Sites of Cytochromes P450 1A1, IIB1, IIB2, and IIE1. *J. Biol. Chem.* **1991**, *266*, 19258–19264.
(19) White, R. E.; McCarthy, M.-B.; Egeberg, K. D.; Sligar, S. G. Regioselectivity in the Cytochromes P450: Control by Protein Constraints and by Chemical Reactivities. *Arch. Biochem. Biophys.* **1984**, *228*, 493–502.
(20) Collins, J. R.; Loew, G. H. Theoretical Study of the Product Specificity in the Hydroxylation of Camphor, Norcamphor, 5,5-Difluorocamphor, and Pericyclocamphenone by Cytochrome $P450_{cam}$. *J. Biol. Chem.* **1988**, *263*, 3164–3170.
(21) Atkins, W. M.; Sligar, S. G. Molecular Recognition in Cytochrome P450: Alteration of Regioselective Alkane Hydroxylation via Protein Engineering. *J. Am. Chem. Soc.* **1989**, *111*, 2715–2717.
(22) Aoyama, T.; Korzekwa, K.; Nagata, K.; Adesnik, M.; Reiss, A.; Lapenson, D. P.; Gillette, J.; Gelboin, H. V.; Waxman, D. J.; Gonzalez, F. J. Sequence Requirements for Cytochrome P450IIB1 Catalytic Activity. *J. Biol. Chem.* **1989**, *264*, 21327–21333.
(23) Furuya, H.; Shimizu, T.; Hatano, T.; Fujii-Kuriyama, Y. Mutations at the Distal and Proximal Sites of Cytochrome $P450_d$ Changed Regio-Specificity of Acetanilide Hydroxylations. *Biochem. Biophys. Res. Commun.* **1989**, *160*, 669–676.
(24) Hanzlik, R. P.; Ling, K.-H. J. Active Site Dynamics of Toluene Hydroxylation by Cytochrome P450. *J. Org. Chem.* **1990**, *55*, 3992–3997.
(25) Korzekwa, K. R.; Jones, J. P.; Gillette, J. R. Theoretical Studies on Cytochrome P450 Mediated Hydroxylation: A Predictive Model for Hydrogen Abstractions. *J. Am. Chem. Soc.* **1990**, *112*, 7042–7046.
(26) Raag, R.; Poulos, T. L. Crystal Structures of Cytochrome $P450_{cam}$ Complexed with Camphane, Thiocamphor, and Adamantane: Factors Controlling P450 Substrate Hydroxylation. *Biochemistry* **1991**, *30*, 2674–2684.
(27) Kronbach, T.; Kemper, B.; Johnson, E. F. A Hypervariable Region of P450IIC5 Confers Progesterone 21-Hydroxylase Activity to P450IIC1. *Biochemistry* **1991**, *30*, 6097–6102.
(28) Novak, R. F.; Vatsis, P. V. ^1H Fourier Transform Nuclear Magnetic Resonance Relaxation Rate Studies on the Interaction of Acetanilide with Purified Isozymes of Rabbit Liver Microsomal Cytochrome P450 and Cytochrome b_5. *Mol. Pharmacol.* **1982**, *21*, 701–709.
(29) Woldman, Y. Y.; Weiner, L. M.; Lyakhovich, V. V. Different Structure of the Complexes of Two Cytochrome P-450 Isozymes with Acetanilide by ^1H-NMR Relaxation and Spectrophotometry. *Biochem. Biophys. Res. Commun.* **1993**, *193*, 40–46.
(30) Crull, G. B.; Kennington, J. W.; Garber, A. R.; Ellis, P. D.; Dawson, J. H. ^{19}F Nuclear Magnetic Resonance as a Probe of the Spatial Relationship Between the Heme Iron of Cytochrome P450 and Its Substrate. *J. Biol. Chem.* **1989**, *264*, 2649–2655.
(31) Poulos, T. L.; Finzel, B. C.; Howard, A. J. High Resolution Crystal Structure of Cytochrome $P450_{cam}$. *J. Mol. Biol.* **1987**, *195*, 687–700.
(32) Paulsen, M. D.; Ornstein, R. L. Substrate Mobility in Thiocamphor-bound Cytochrome $P450_{cam}$: An Explanation of the Conflict Between the Observed Product Profile and the X-ray Structure. *Protein Eng.* **1993**, *6*, 359–365.
(33) Hinson, J. A.; Mitchell, J. R. *N*-Hydroxylation of Phenacetin by Hamster Liver Microsomes. *Drug Metab. Dispos.* **1976**, *4*, 430–435.
(34) Astrom, A.; DePierre, J. W. Metabolism of 2-Acetyl-aminofluorene by Eight Different Forms of Cytochrome P450 Isolated from Liver. *Carcinogenesis* **1985**, *6*, 113–120.
(35) McManus, M. E.; Burgess, W. M.; Veronese, M. E.; Huggett, A.; Quattrochi, L. C.; Tukey, R. H. Metabolism of 2-Acetylaminofluorene and Benzo[a]pyrene and Activation of Food-derived Heterocyclic Mutagens by Human Cytochromes P450. *Cancer Res.* **1990**, *50*, 3367–3376.
(36) Loew, G. H.; Goldblum, A. Metabolic Activation and Toxicity of Acetaminophen and Related Analogs. *Mol. Pharmacol.* **1985**, *27*, 375–386.
(37) Hoffman, K.-J.; Axworthy, D. B.; Baillie, T. A. Mechanistic Studies on the Metabolic Activation of Acetaminophen *In Vivo*. *Chem. Res. Toxicol.* **1990**, *3*, 204–211.
(38) Nelson, S. D.; Forte, A. J.; Vaishnev, Y.; Mitchell, J. R.; Gillette, J. G.; Hinson, J. A. The Formation of Arylating and Alkylating Metabolites of Phenacetin in Hamsters and Hamster Liver Microsomes. *Mol. Pharmacol.* **1981**, *19*, 140–145.
(39) Baillie, T. A.; Tirmenstein, M. A.; Nelson, S. D. Unpublished results.
(40) Ottoboni, S.; Carlson, T. J.; Trager, W. F.; Castagnoli, K.; Castagnoli, N., Jr. Studies on the Cytochrome P450 Catalyzed Ring α-Carbon Oxidation of the Nigrostriatal Toxin 1-Methyl-4-phenyl-1,2,3,6-tetrahydropyridine (MPTP). *Chem. Res. Toxicol.* **1990**, *3*, 423–427.
(41) Sugiyama, K.; Yao, K.; Rettie, A. E.; Correia, M. A. Inactivation of Rat Hepatic Cytochrome P450 Isozymes by 3,5-Dicarbethoxy-2,6-dimethyl-4-ethyl-1,4-dihydropyridine. *Chem. Res. Toxicol.* **1989**, *2*, 400–410.
(42) Waxman, D. J.; Walsh, C. Phenobarbital-induced Rat Liver Cytochrome P450. *J. Biol. Chem.* **1982**, *257*, 10446–10457.
(43) Lowry, O. H.; Rosebrough, N. J.; Farr, A. L.; Randall, R. J. Protein Measurement with the Folin Phenol Reagent. *J. Biol. Chem.* **1951**, *193*, 265–275.
(44) Omura, T.; Sato, R. The Carbon Monoxide-binding Pigment of Liver Microsomes. *J. Biol. Chem.* **1964**, *239*, 2370–2378.
(45) Mildvan, A. S.; Gupta, R. K. Nuclear Relaxation Measurement of the Geometry of Enzyme-bound Substrates and Analogs. *Methods Enzymol.* **1978**, *49*, 322–359.
(46) Berton, D. R.; Sture, F.; Karlstrom, G.; Dewk, R. A. Proton Relaxation Enhancement (PRE) in Biochemistry: A critical survey. *Prog. NMR Spectrosc.* **1979**, *13*, 1–45.
(47) Craik, D. J.; Higgins, K. A. NMR Studies of Ligand-Macromolecule Interactions. *Annu. Rep. NMR Spectrosc.* **1989**, *22*, 61–138.
(48) Rag, B. D.; Rosch, P.; Rao, B. D. N. ^{31}P NMR Studies of the Structure of Cation Nucleotide Complexes Bound to Porcine Muscle Adenylate Kinase. *Biochemistry* **1988**, *27*, 8669–8676.
(49) Shoemaker, D. P.; Garland, C. W.; Steinfeld, J. I. *Experiments in Physical Chemistry*, 3rd ed.; McGraw-Hill: New York, 1974; pp 52–54.